

Computer Simulation of Crystallization from Solution

Jamshed Anwar* and Papa Kofi Boateng

Contribution from the Computational Pharmaceutical Sciences Laboratory, Department of Pharmacy, King's College London, Manresa Road, London SW3 6LX, U.K.

Received August 7, 1997. Revised Manuscript Received July 20, 1998

Abstract: The early stages of crystallization are not fully understood, a particularly challenging problem being crystallization from solution. The processes involved at an atomic level remain elusive to experiment. Furthermore, crystallization from solution has been thought to be inaccessible by atomistic computer simulations. This study demonstrates that crystallization from solution can in fact be simulated using the method of molecular dynamics for a model solute/solvent system consisting of atomic species characterized by the Lennard-Jones potential function. The model has been applied to look at the effects of varying supersaturation and of inclusion of a simple inhibitor in the system. The behavior of the model is in accord with experiment. In general, increasing supersaturation causes earlier onset of crystallization. Crystallization in highly supersaturated systems involves liquid–liquid phase separation followed by nucleation in the solute phase. The nucleation event in such systems does not appear to be influenced by the solvent. Inclusion of inhibitors retards the onset. Additionally, extensive solute clustering is observed. The crystallization model and variations on it, as well as step by step extension to realistic systems, should enable further testing and development of theory of crystal nucleation and growth and provide insights of technological importance.

Introduction

Crystal nucleation and growth is central to many processes in both living organisms and the inanimate world. To be able to understand, control, optimize, and predict this phenomena and its consequences is highly desirable. The crystal structure, morphology, and size as well as the crystal quality can affect the chemical reactivity, bulk powder flow, rheology and stability of suspensions, and other mechanical and physical properties of a substance. Consequently this technology is of considerable importance to a whole host of industries including photographic chemicals, agrochemicals, dyestuff, specialty chemicals, and pharmaceuticals. For pharmaceuticals an appropriate choice of crystal form can enhance the bioavailability of the drug.¹ Notable biological examples of interest include biomineralization of bone, teeth, and shells² (a better understanding of which would be useful for interfacing biominerals with inorganic orthopaedic implants), deposition of uric acid crystals in the clinical condition of gout, and the mechanism of action of antifreeze proteins.³ Finally, a greater understanding of crystal nucleation and growth processes promises a new class of functional solids based on self-assembly of designed molecules.⁴

Despite all the interest, the mechanics of crystallization still remain an important fundamental problem.⁵ The essential difficulty is that the processes taking place at the atomic scale are barely or not at all accessible to current experimental methods. Consequently one has had to resort to models, both physical and theoretical. Of the physical models, the hard sphere

colloids have perhaps given the most insight.⁶ The second viable alternative is numerical computer simulations based on the atom–atom potential method.⁷ Static potential energy calculations based on this approach have, to a limited extent, been useful in predicting morphology and for rationalizing the effects of crystal growth inhibitors.⁸ Explicit computer simulations (using the Monte Carlo and the molecular dynamics techniques⁹) of the crystallization process have been carried out, but these have been restricted to investigating crystallization from the melt.^{10–16} These studies support the classical ideas of crystal nucleation and growth: the importance of the critical size of a germ nucleus and the existence of a free energy barrier and its variation as a function of supercooling.

For technological purposes crystal growth from solution is the method of choice. This process, however, is considered to be as yet outside the scope of computer simulation because of

(6) (a) Pusey, P. N.; van Megan, W. *Nature* **1986**, *320*, 340–342. (b) van Megan, W.; Underwood, S. M. *Nature* **1993**, *362*, 616–618. (c) Harland, J. L.; Henderson, S. J.; Underwood, S. M.; van Megan, W. *Phys. Rev. Lett.* **1995**, *75*, 3572–3575. (d) Zhu, J.; Li, M.; Rogers, R.; Meyer, W.; Ottewill, R. H.; Russell, W. B.; Chaikin, P. M. *Nature* **1997**, *387*, 883–885. (e) van Blaaderen, A.; Ruel, R.; Wiltzius, P. *Nature* **1997**, *385*, 321–324.

(7) Pertsin A. J.; Kitaigorodsky A. I. *The Atom-Atom Potential Method*. Springer Ser. Chem. Phys. **1987**, *43*.

(8) Docherty, R.; Clydesdale, G.; Roberts, K. J.; Bennema, P. *J. Phys. D: Appl. Phys.* **1991**, *24*, 89–99.

(9) Allen, M.; Tildesley, D. *Computer Simulation of Liquids*; Oxford Science Publications: Oxford, U.K., 1987.

(10) Esselink, K.; Hilbers, P. A. J.; van Beest, B. W. H. *J. Chem. Phys.* **1994**, *101*, 9033.

(11) Mandell, M. J.; McTague, J. P.; Rahman, A. *J. Chem. Phys.* **1976**, *64*, 3699.

(12) Mandell, M. J.; McTague, J. P.; Rahman, A. *J. Chem. Phys.* **1977**, *66*, 3070.

(13) Swope, W. C.; Andersen, H. C. *Phys. Rev. B* **1990**, *41*, 7042.

(14) van Duijneveldt, J. S.; Frenkel, D. *J. Chem. Phys.* **1992**, *96* (6), 4655.

(15) ten Wolde, P. R.; Ruiz-Montero, M. J.; Frenkel, D. *J. Chem. Phys.* **1996**, *104* (24), 9932.

(16) Nosé, S.; Yonezawa, F. *J. Chem. Phys.* **1986**, *84* (3), 1803.

* To whom correspondence should be addressed. E-mail: jamshed.anwar@kcl.ac.uk.

(1) Haleblan, J.; McCrone, W. *J. Pharm. Sci.* **1969**, *58*, 911.

(2) (a) Mann, S.; Ozin, G. A. *Nature* **1996**, *382*, 313–318. (b) Mann, S.; Walsh, D. *Chem. Br.* **1996** (Nov), 31–34.

(3) Sicheri, F.; Yang, D. S. C. *Nature* **1995**, *375*, 427–431.

(4) (a) Ball, P. *Nature* **1996**, *381*, 648–650. (b) Stupp, S. I.; LeBonheur, V.; Walker, L. S. L.; Huggins, K. E.; Keser, M.; Amstutz, A. *Science* **1997**, *276*, 384–389.

(5) Maddox, J. *Nature* **1995**, *378*, 231.

the long time scales involved and the requirement of a large system size.¹⁷ A possible fruitful approach is to move away from realistic systems to much simpler models of solute and solvent, for which the crystallization time scale may be shorter and accessible to computer simulation. Indeed, the challenge has been the identification of such a simple model. The model must be such that at the defined temperature and pressure only the solute crystallizes with the solvent remaining in the liquid state. Technically this implies the identification of appropriate force field parameters to describe the solute–solute, solute–solvent, and solvent–solvent interactions.

Here we report that crystallization from solvent can in fact be simulated using the method of molecular dynamics for a model solute–solvent system consisting effectively of atoms of two noble gases with one dissolved in the other. The thermodynamic conditions of temperature and pressure are chosen such that one of the species, the solute, is in the solid phase, while the other, the solvent, is in the liquid phase. The atomic species are characterized by the Lennard-Jones potential function. The key to our success has been the well-characterized phase diagram of the Lennard-Jones (LJ) particle system.¹⁸ From the LJ phase diagram it is possible to select appropriate force field parameters that define particles as either solid, liquid, or gas at a given temperature and pressure. We illustrate the effectiveness of the model with preliminary results from studies investigating the effects of supersaturation on crystal nucleation and growth, the action of crystallization inhibitors, and the existence of clusters in supersaturated solutions. All in all, the behavior is not that far removed from real systems. This proposed model and variations on it, as well as the step by step development of realistic solute–solvent systems, will enable testing of current theoretical ideas and aid further development of theory of crystal nucleation and growth. The insights gained will be invaluable for rationally engineering crystals of technological importance.

Methodology

Molecular dynamics simulations of the LJ solute/solvent particles were carried out in the constant-temperature (Nose¹⁹–Hoover²⁰ thermostat) constant-pressure ensemble using the computer program DLPOLY.²¹ Isotropic periodic boundary conditions were employed. The time step was 4 fs, while the mass for both the solute and solvent particles was set to 5 g/mol. This low value for mass ensured greater sampling of phase space. The mass is, of course, coupled to the optimum time step; excessively low particle mass combined with large time steps can lead to gross errors in the simulation trajectories. The concentration of the solute particles in the solution was generally kept fixed at about 15%. All simulations were started with the solute particles interdispersed in the solvent in an NaCl-type cubic lattice. The simulations were carried out for periods of 150 ps. System size was typically about 500 solute and 3000 solvent particles. Simulations using large systems containing a varying amount of solute particles were also carried out. These had about 2500 solute/16 000 solvent and 1000 solute/16 000 solvent particles. The cutoff for the atom interactions was about $3.5\sigma_{\max}$, where σ_{\max} was the maximum LJ σ in the system. Typically the cutoff amounted to 15.5 Å. The selected LJ force field parameters for the solute and solvent particles are given in Table 1. The solute–solute parameters characterize a solid phase, while the solvent–solvent parameters characterize the liquid phase at the chosen temperature and pressure conditions of 300 K and 0.77 kbar.

Table 1. Lennard-Jones Parameters for the Solute and Solvent Particles

interaction	$\epsilon/\text{kJ mol}^{-1}$	$\sigma/\text{Å}$
solute–solute	8.314	4.48
solvent–solvent	2.494	3.00
solute–solvent	4.0–0.01	3.74

The unlike interactions, in this case solute–solvent, are normally calculated using the Lorentz–Berthelot mixing rules:

$$\sigma_{\text{solute-solvent}} = \frac{1}{2}(\sigma_{\text{solute-solute}} + \sigma_{\text{solvent-solvent}})$$

$$\epsilon_{\text{solute-solvent}} = (\epsilon_{\text{solute-solute}}\epsilon_{\text{solvent-solvent}})^{1/2}$$

In this study $\sigma_{\text{solute-solvent}}$ was determined by this method. However, the choice of the LJ ϵ parameter characterizing the solute–solvent interaction is critical to this study. This parameter defines the affinity between the two particle types. A low value implies low affinity and thus a low solubility of the solute in the solvent, while a high value is indicative of a high affinity and therefore high solubility. Hence, for a system in which the ratio of solute to solvent particles is fixed, the value of $\epsilon_{\text{solute-solvent}}$ defines the extent of saturation or supersaturation. Low values of $\epsilon_{\text{solute-solvent}}$ would yield a more supersaturated solution. The effect of varying the supersaturation was explored by carrying out systematic simulations in which the percentage of solute particles was kept fixed, with the variation in effective supersaturation being achieved by varying the $\epsilon_{\text{solute-solvent}}$ parameter from 0.01 to 4.0 kJ mol⁻¹. Using the Lorentz–Berthelot rules $\epsilon_{\text{solute-solvent}}$ would correspond to 4.5 kJ mol⁻¹.

In view of the technological importance of crystallization inhibitors, a preliminary study was carried out to examine the effect of a designer inhibitor molecule on the rate of crystallization for the LJ system. The inhibitor molecule was a dimer with both atoms having force field parameters of solute particles with one of the atoms being larger having a LJ σ parameter of 1.5 times that of the solute. The Lorentz–Berthelot rules were used to describe the interaction between solute and inhibitor particles. For the inhibitor–solvent interaction, the LJ $\sigma_{\text{inhibitor-solvent}}$ parameter was calculated using the Lorentz–Berthelot combining rule while the LJ $\epsilon_{\text{inhibitor-solvent}}$ parameter was taken to be the same as the $\epsilon_{\text{solute-solvent}}$ interaction.

Results and Discussion

Snapshots of the solute/solvent system at various stages of the simulation are shown in Figure 1. Upon starting the simulations, the initial starting lattice breaks down almost immediately. The solute particles tend to aggregate into small clusters which then come together to form a single large cluster. The cluster then nucleates and crystallizes. The eventual crystallite is largely spherical but shows rudimentary facets. The spherical morphology, however, is only observed in the larger system sizes, being grossly modified, in the smaller system size, by the effects of the periodic boundary conditions employed in the simulations. This problem is particularly acute in systems with high solute concentrations, where the crystalline structure elongates in one direction and spans both ends of the simulation box in an effort to minimize the surface energy.

A typical radial distribution function, $g(r)$, for the solute–solute particles as a function of time is shown in Figure 2 with each $g(r)$ averaged over 4 ps. It clearly indicates the breakdown of the starting lattice and then the crystallization. The corresponding solvent–solvent $g(r)$, which categorically confirms that the structure of the solvent particles remains liquid throughout the simulation, is also shown in Figure 2. Closer examination of the solute–solute $g(r)$ reveals two distinct stages. First there is an immediate breakdown of the starting configuration. This is followed by the emergence of some rather broad peaks at 8.5, 9.5, and 12.7 Å indicative of a diffuse structure.

(17) Boek, E. S.; Briels, W. J.; Feil, D. *J. Phys. Chem.* **1994**, *98*, 1674.

(18) Agrawal, R.; Kofke, D. A. *Mol. Phys.* **1995**, *85*, 43.

(19) Nosé, S. *Mol. Phys.* **1984**, *52*, 255.

(20) Hoover, W. G. *Phys. Rev.* **1985**, *A31*, 1695.

(21) DLPOLY: Parallel molecular dynamics program; Developed and distributed by the Theory Group, CLRC Daresbury Laboratory, Warrington, Cheshire, U.K.

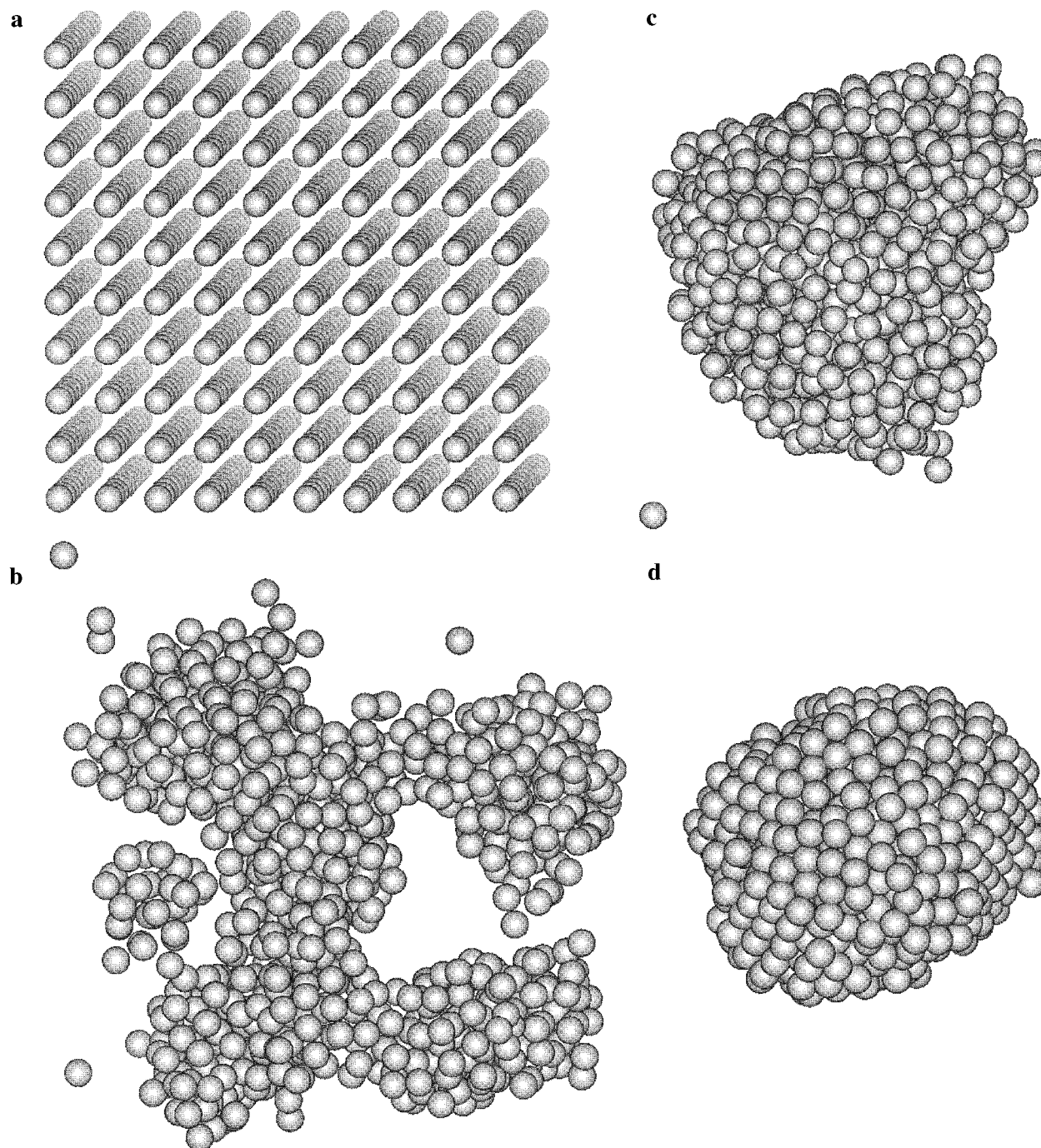


Figure 1. Snapshots of the simulation system containing 1000 solute and 16 384 solvent particles as a function of time. For clarity only the solute particles are shown: (a) initial starting configuration in which the solute particles are interdispersed in the solvent particles, (b) 6 ps, (c) 16 ps, and (d) 140 ps into the simulation. The LJ parameters for the solute–solvent interaction were $\epsilon = 1.0 \text{ kJ mol}^{-1}$ and $\sigma = 3.74 \text{ \AA}$.

The diffuse structure persists from about 20 to 70 ps and is then supplanted by the final crystalline phase. This is best described by Figure 3, which shows four time zones in the development of the crystalline phase. The existence of a diffuse precursor phase is a highly notable event and could lend considerable support to Ostwald's rule of stages.²² According to Ostwald's rule, the structure that crystallizes first is that which has the lowest energy barrier (thus highest energy). This form would then transform to the next lower energy form and so on. The $g(r)$ of the diffuse phase is not consistent with that of any *pure* cubic phase but appears to contain peaks for both the body-centered cubic (BCC) and the face-centered cubic (FCC) phases.

As to whether there are distinct regions corresponding to each phase within the solute cluster or whether the cluster has a homogeneous structure with characteristics of both BCC and FCC requires more detailed analysis. On the other hand, the final crystalline phase categorically corresponds to the FCC phase. The FCC phase is indeed the stable phase for the force field parameters utilized in present study. This was confirmed by carrying out molecular dynamics simulations of crystals of the FCC, BCC, and hexagonal close packed (HCP) phases in the solid state using the Parrinello–Rahman²³ boundary conditions. In these simulations both the BCC and HCP phases

(22) Ostwald, W. *Z. Phys. Chem.* **1897**, 22, 289.

(23) (a) Parrinello, M.; Rahman, A. *Phys. Rev. Lett.* **1980**, 45, 1196. (b) Parrinello, M.; Rahman, A. *J. Appl. Phys.* **1981**, 52, 7182.

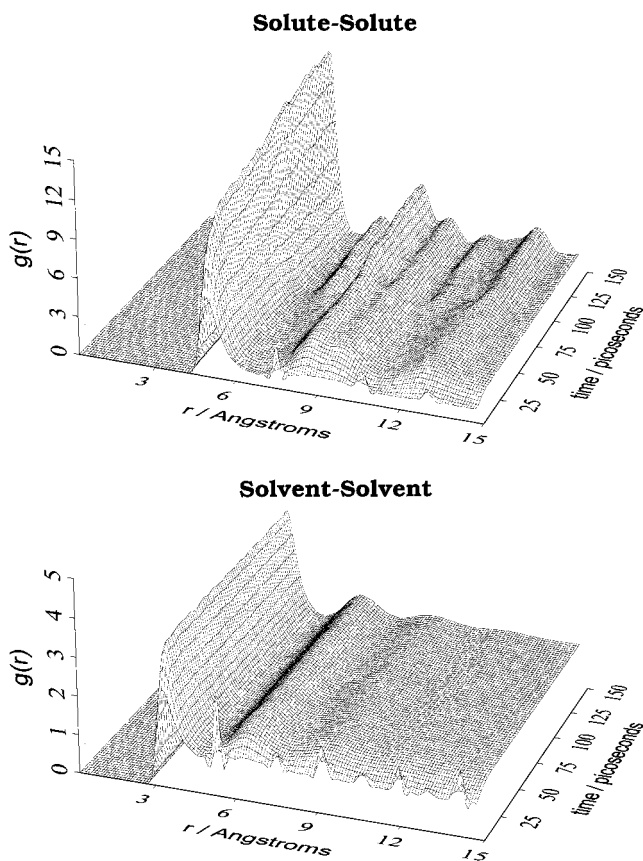


Figure 2. Radial distribution function (RDF) of the solute and solvent particles as a function of simulation time. Each RDF is averaged over 4 ps. With increasing simulation time the RDF of the solute particles takes the characteristic form (well-defined peaks) of a crystal, while that of the solvent particles remains characteristic of a liquid. The RDF of the resulting crystalline phase corresponds to face-centered cubic packing. The LJ parameters for the solute–solvent interaction were $\epsilon = 1.0 \text{ kJ mol}^{-1}$ and $\sigma = 3.74 \text{ \AA}$.

transformed almost immediately to the FCC phase, while the FCC starting phase remained stable. The FCC phase has also been observed to be the stable phase in simulation studies of crystallization from the melt.^{11–16} These observations in which crystallization is preceded with a diffuse precursor phase (with some characteristics of a BCC phase) followed by eventual crystallization of an FCC phase add strong support to Ostwald's rule. Pre-critical nuclei with a BCC-like structure which subsequently transform to the more stable FCC structure have also been observed in simulations of crystallization from melt.¹⁵

Consider now the effects of varying the effective supersaturation. Table 2 shows the variation of onset of crystallinity, as determined by the time of appearance of the second peak (at 7.1 Å) in the radial distribution function for the solute–solvent interaction, as a function of the LJ $\epsilon_{\text{solute-solvent}}$ parameter. A low value of $\epsilon_{\text{solute-solvent}}$ defines a system with very low solubility, and with a fixed concentration of solute of about 15%, the resultant solution is, in relative terms, supersaturated. At the lower supersaturations, corresponding to $\epsilon_{\text{solute-solvent}}$ values above 2.0 kJ mol^{-1} , the solute particles remained intermixed with the solvent particles with no clustering or crystallization. At $\epsilon_{\text{solute-solvent}}$ values of 2.0 kJ mol^{-1} the solute molecules were observed to aggregate but not crystallize over the time scale of the simulation. At all $\epsilon_{\text{solute-solvent}}$ values below 2.0 kJ mol^{-1} (corresponding to very high supersaturations) the solute crystallized. The onset of crystallization became earlier as the magnitude of the LJ $\epsilon_{\text{solute-solvent}}$ parameter decreased, with a

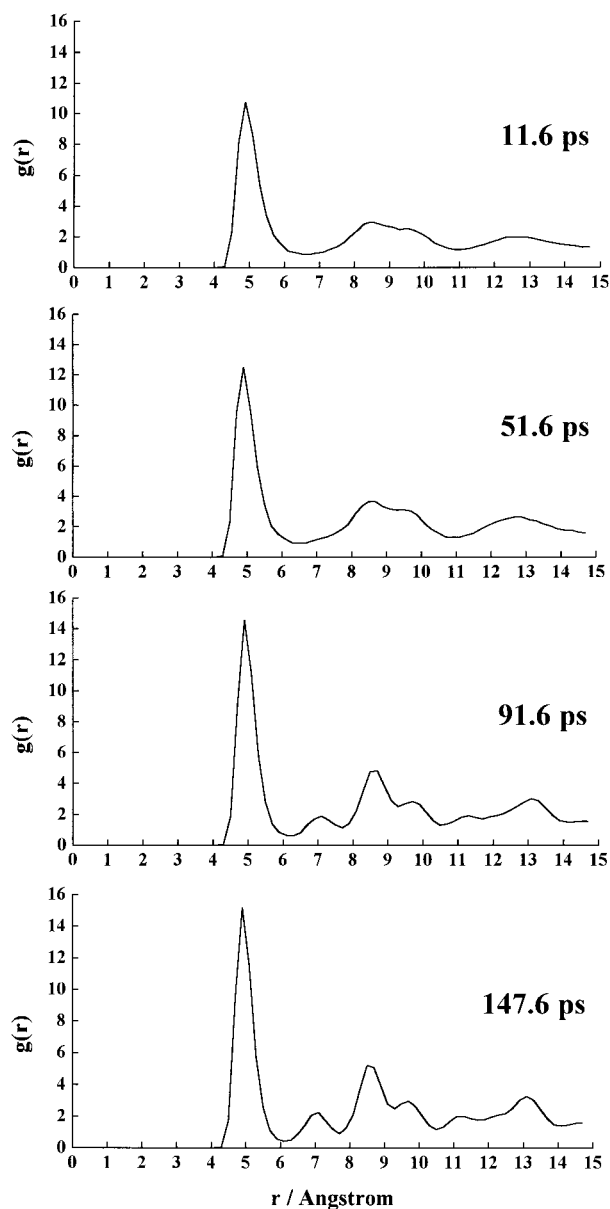


Figure 3. Radial distribution function (RDF) of the solute particles at selected simulation times. Each RDF is averaged over 4 ps. The LJ parameters for the solute–solvent interaction were $\epsilon = 1.0 \text{ kJ mol}^{-1}$ and $\sigma = 3.74 \text{ \AA}$.

Table 2. Onset of Crystallization as Determined by the Time of Appearance of the Second Peak (at 7.1 Å) in the Radial Distribution Function for the Solute–Solvent Interaction as a Function of LJ

$\epsilon_{\text{Solute-Solvent}}$			
LJ $\epsilon_{\text{solute-solvent}}$ (kJ mol^{-1})	onset of crystallization (ps)	LJ $\epsilon_{\text{solute-solvent}}$ (kJ mol^{-1})	onset of crystallization (ps)
4.0	no crystallization	0.1	61.6
3.0	no crystallization	0.05	39.6
2.0	no crystallization	0.01	31.6
1.0	73.6	0.005	47.6
0.5	57.6		

limiting value around 0.01 kJ mol^{-1} . Below this value the onset of crystallization appears to become delayed. The cause for the delay at the very low values of $\epsilon_{\text{solute-solvent}}$ is a little uncertain. It could result from an increase in the effective pressure (resulting from the high solute–solvent interfacial energy) within the cluster which retards the motion of the atoms past each other. However, for the very small values of

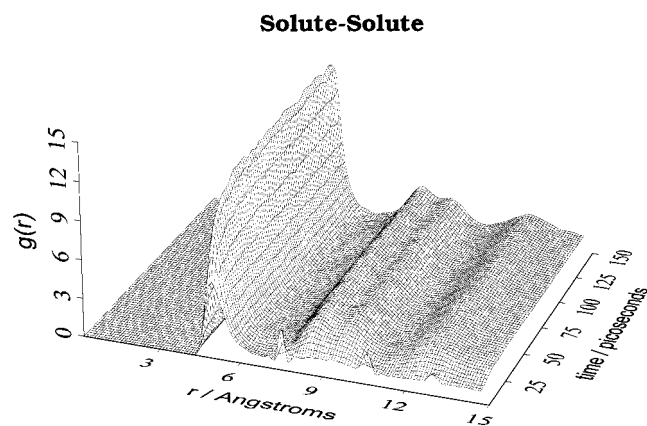


Figure 4. Radial distribution function (RDF) of the solute particles in a system comprising 457 solute and 2687 solvent particles and 24 dimer inhibitor molecules as a function of simulation time. This RDF can be directly compared with that in Figure 2 which characterizes the same system without any inhibitor molecules present. The inhibitor molecules are clearly effective in inhibiting crystallization.

$\epsilon_{\text{solute-solvent}}$, a decrease in the effective hard-core radius means a decrease in the excluded volume, giving rise to an increase in the solubility hence a decrease in supersaturation. The overall behavior of the simulated system seems to be consistent with experimental observations on real systems: the rate of crystallization increasing with increase in supersaturation. In real systems very high supersaturations cause rapid precipitation of an amorphous product. If, as $\epsilon_{\text{solute-solvent}}$ is reduced, the effects of the decrease in the excluded volume is such that there is still an overall increase in supersaturation, then the delay in crystallization at the very low $\epsilon_{\text{solute-solvent}}$ is akin to the production of an amorphous product.

The formation of aggregates and clustering in systems with $\epsilon_{\text{solute-solvent}}$ values of 2.0 kJ mol^{-1} also has important parallels with experiment. This feature of the simulations adds considerable weight to the idea that there is extensive solute association and cluster formation in supersaturated solutions.²⁴ The existence of pre-nucleation clusters has been proposed to explain a number of experimental observations. These observations include the existence of concentration gradients in columns of supersaturated solutions,²⁵⁻²⁷ and the rapid and massive crystallization of quiescent supersaturated solutions on agitation or introduction of a foreign body.^{24,28} Essential to the explanation of the latter effect is the existence of clusters with a structure that is very close to that of the resulting crystals.

The simulations also shed some light on the nucleation process in highly supersaturated solutions. Since, in these

(24) Larson, M. A. In *Advances in Industrial Crystallization*; Garside, J., Davey, R. J., Jones, A. G., Eds.; Butterworth-Heinemann: Oxford, U.K., 1991; p 20.

(25) Mullin, J. W.; Leci, C. *Philos. Mag.* **1969** *19*, 1075.

(26) Allen, A. T.; McDonald, M. P.; Nicol, W. M.; Wood, R. M. *Nature Physical Sciences* **1972**, 235, 36.

(27) Larson, M. A.; Garside, J. J. *Cryst. Growth* **1986**, 76, 88.

(28) Rusli, I. T. Solute clustering and crystallization from solution. Ph.D. Thesis, Iowa State University, 1988.

(29) Desiraju, G. R. *Crystal Engineering*; Elsevier: Amsterdam, 1989.

(30) Davey, R. J.; Maginn, S. J.; Andrews, S. J.; Buckley, A. M.; Cottier, D.; Dempsey, P.; Rout, J. E.; Stanley, D. R.; Taylor, A. *Nature* **1993**, 366, 248.

(31) York, P. *Drug Dev. Ind. Pharm.* **1992**, 18, 677.

(32) Weissbuch, I.; Popovitz-Biro, R.; Lahav, M.; Leiserovitz, L. *Acta Crystallogr.* **1995**, B51, 115.

systems, clustering precedes nucleation, the nucleation event occurs within the cluster and is not expected to be influenced by the solvent. The implication is that the mechanics of nucleation in highly supersaturated solutions are no different from nucleation taking place in the melt. Indeed such ideas have been expressed earlier,²⁴ though with little evidence. From these studies one could extrapolate to macroscopic systems. An immediate suggestion arising might be that the system would separate into two distinct phases and the solute then crystallizes. However, there are at least two competing kinetic processes that will determine the outcome: the rate of coarsening of the mixture into the two phases and the rate of crystal nucleation. If the latter is dominant, then nucleation and growth of the crystalline phase will occur well before any significant coarsening and/or bulk separation of the two phases. Regions of the separated solute phase will crystallize to yield individual crystallites. Such observations would be consistent with experiment: rapid crystallization from highly supersaturated solutions invariably yield numerous discrete crystallites. Clearly, very large scale simulations are required to resolve this issue.

A thorough understanding of the nucleation and crystal growth process is invaluable to developing technology for inhibiting crystallization and engineering crystals with desired properties.²⁹⁻³¹ An important approach to inhibiting crystallization and engineering crystals is the use of "tailor-made" additives.³² The effective inhibitors are those that have some aspect of the structure that resembles the solute molecules coupled with a moiety that is structurally very different from the solute. This latter either terminates some directional polar interactions or may give rise to steric hindrance. It may even be a long-chain polymer. The inhibitor is thought to attach itself to the growing nuclei/crystal and then prevent the subsequent attachment of further solute molecules/atoms. The results of the preliminary study in which model inhibitor molecules were added to the system are encouraging. The $g(r)$ as a function of time of the system with the dimer inhibitor molecule is shown in Figure 4 and can be directly compared with Figure 2. The onset of crystallization is totally inhibited over the time scales of the simulation compared with the system in which there was no inhibitor present. The inhibitor molecules added are retained within the solute cluster, preventing the formation of a stable structure. These observations clearly confirm the effectiveness of the LJ particle system as a model for crystallization from solution. Systematic studies with dimer, bidentate, and other inhibitor structures are underway to look at the mechanism of inhibition.

In conclusion, a computer simulation model based on atomic species characterized by the Lennard-Jones potential function has been developed for modeling crystallization from solution. The effectiveness of the model has been demonstrated by examining the effects of supersaturation on crystal nucleation and growth and of the inclusion of inhibitor molecules within the system. Crystallization in highly supersaturated solutions has been found to involve liquid-liquid phase separation followed by nucleation in the solute phase.

Acknowledgment. We thank a reviewer for bringing to our attention the significant reduction in the excluded volume in the solute-solvent interaction at the very low values of the LJ parameter $\epsilon_{\text{solute-solvent}}$.

JA972750N